Research article

Arabidopsis katanin binds microtubules using a multimeric microtubule-binding domain

Virginie Stoppin-Mellet [a], Jérémie Gaillard [a], Ton Timmers [b], Emmanuelle Neumann [c], James Conway [c,1], Marylin Vantard [a,*]

[a] *Laboratoire de Physiologie Cellulaire Végétale, UMR 5168, CNRS/CEA/INRA/Université Joseph Fourier, Institut de Recherches en Sciences et Technologies pour le Vivant, 17 rue des Martyrs, F-38054 Grenoble Cedex 9, France*
[b] *Laboratoire des Interactions Plantes Micro-organismes, UMR 2594 CNRS/INRA, Chemin de Borde Rouge, BP 52627, F-31326 Castanet Tolosan Cedex, France*
[c] *Institut de Biologie Structurale UMR 5057 CEA/CNRS/UJF, 41 rue Jules Horowitz, 38027 Grenoble, France*

Abstract

Katanin is a heterodimeric protein that mediates ATP-dependent destabilization of microtubules in animal cells. In plants, the catalytic subunit of *Arabidopsis thaliana* katanin (AtKSS, *Arabidopsis thaliana* Katanin Small Subunit) has been identified and its microtubule-severing activity has been demonstrated in vitro. In vivo, plant katanin plays a role in the organization of cortical microtubules, but the way it achieves this function is unknown. To go further in our understanding of the mechanisms by which katanin severs microtubules, we analyzed the functional domains of *Arabidopsis* katanin. We characterized the microtubule-binding domain of katanin both in vitro and in vivo. It corresponds to a poorly conserved sequence between plant and animal katanins that is located in the N-terminus of the protein. This domain interacts with cortical microtubules in vivo and has a low affinity for microtubules in vitro. We also observed that katanin microtubule-binding domain oligomerizes into trimers. These results show that, besides being involved in the interaction of katanin with microtubules, the microtubule-binding domain may also participate in the oligomerization of katanin. At the structural level, we observed that AtKSS forms ring-shaped oligomers.
© 2007 Elsevier Masson SAS. All rights reserved.

Keywords: Katanin; Microtubule-binding domain; Oligomerization; Severing of microtubules

1. Introduction

Plant microtubules are located in the cell cortex (cortical microtubules during interphase, preprophase band at the entry of mitosis) and in the cytoplasm (nucleus-associated microtubules, spindle and phragmoplast microtubules in mitosis), where they are arranged in highly dynamic and ordered arrays.

Upon internal and external stimuli, these arrays reorganize, while acquiring specific functions including the equal segregation of chromosomes, the formation of the cell plate at the end of mitosis, the transport of cargo and the positioning of organelles [1,2]. The architectural changes of these microtubule arrays are dramatic manifestations of the flexibility and dynamic turnover of the microtubules in plant cells. The precise mechanisms underlying the remodeling of microtubule arrays remain difficult to elucidate, mainly because of the complexity of the plant microtubular cytoskeleton and because of the absence in plant cells of a discrete microtubule-organizing center. When compared with animal microtubules, plant microtubules possess very peculiar properties in vivo [3–6], including the fact that cortical microtubules exhibit polymerization-biased

---

dynamic instability at one end and slow depolymerization at the other end [5].

In vivo, the control of microtubule assembly and disassembly requires a multitude of adaptors and regulators. These proteins associate with the polymer lattice, with the microtubule ends or with the tubulin dimer. They regulate microtubule stabilization or destabilization in a way to generate the different microtubule arrays observed in vivo [7,8]. Until recently the identification of plant microtubule regulators has been rather elusive because of their low abundance and because most of them show low sequence homology with animal counterparts. Several plant microtubule-stabilizing effectors, also called Microtubule Associated Proteins, have now been identified and their functional characterization is under way [9,10]. So far, AtKSS (*Arabidopsis thaliana* Katanin Small Subunit) is the only plant microtubule-destabilizing protein that has been functionally characterized.

Katanin is a heterodimer composed of a catalytic subunit of 60 kDa (p60) that hydrolyses ATP to sever microtubules, and a regulatory subunit of 80 kDa (p80) involved in subcellular targeting of katanin [11,12]. p60 oligomerizes into a ring-shaped hexamer in an ATP-dependent process, which is coupled to the disassembly of microtubules [13]. In animal cells, katanin is located at the centrosomes and at spindle poles where it controls the length of the mitotic spindle [14,15]. In plants, the *Arabidopsis* homologue of katanin catalytic subunit, named AtKSS, was identified on the basis of its sequence similarity with human (*Homo sapiens*) and sea urchin katanins [16]. In vitro, AtKSS has a microtubule-stimulated ATPase activity and severs microtubules in an ATP-dependent manner [17]. In vivo, properties and functions of plant katanin are not well understood. Over the last few years, five AtKSS mutants have been described. *botero1* (*bot1*) is a null mutant [18], while the four other mutants, *fragile fiber* (*fra2* [19,20]), *ectopic root hair 3* (*erh3* [21]), *LUC-super-expressor 1* (*lue1* [22]), *dwarf and gladius leaf1* (*dgl1* [23]) are mutated in the C-terminal ATPase domain of AtKSS. All these mutants show a common dwarf phenotype associated with an alteration of cellular anisotropic growth. But a closer look at the plants revealed differences between the mutants. For example, both *fra2* and *lue1* show altered composition and organization of cellulose microfibrils, as well as two-branched trichomes, whereas none of these two defects was observed in *bot1*. Similarly, some but not all cells of *bot1*, *dgl1*, *fra2* and *lue1* have disorganized cortical microtubules. Because of the complexity and the diversity of the phenotypes of AtKSS mutants, it has been difficult to get a clear view of the functions of katanin in vivo. By analyzing the induced expression of AtKSS in *Arabidopsis*, we recently showed that katanin favors bundling of microtubules in the cell cortex [24]. Obviously, AtKSS is required for a proper organization of cortical microtubules in expanding plant cells, but whether the disorganization of cortical microtubule arrays is a direct or indirect consequence of AtKSS's defect is debated.

To further understand the biological roles of AtKSS, we studied the properties of full-length and truncated AtKSS both in vitro and in vivo. We report here that AtKSS interacts with microtubules through a poorly conserved basic domain, both in vitro and in vivo. We observed that AtKSS organized into ring-shape structures, and that the microtubule-binding domain of AtKSS formed trimers. These results suggest that the microtubule-binding domain of AtKSS participate in the oligomerization of plant katanin.

2. Methods

2.1. Chemicals and antibodies

Unless specified, all chemicals were purchased from Sigma (St Louis, MO, USA). GST antibodies were purchased from Amersham Pharmacia Biotech (Little Chalfont, UK). Anti-AtKSS antibodies raised against the N-terminus peptide of the protein were previously described [17].

2.2. AtKSS cloning and expression

Three domains of AtKSS were defined: the 34 first amino acids (aa) (domain 1), aa 35 to 210 (domain 2) and the ATPase domain (aa 211 to 523; domain 3). These domains are further referred to as AtKSS1, AtKSS2 and AtKSS3 respectively. AtKSS1, AtKSS2, AtKSS3, as well as combinations of the domains, AtKSS12 (aa 1 to 210), and AtKSS23 (aa 211 to 523), were cloned into the pGEX-4T-1 plasmid (Amersham Pharmacia Biotech) using BamHI and EcoRI restriction sites, in frame with the glutathione *S*-transferase (GST) (Amersham Pharmacia Biotech) using the following primers: for AtKSS1, primers 5HAtKSS60 5′-CGCGGATCCGTGGGAAGTAGTAAT-3′ and R34 5′-CCCGAATTCTTAGAAGAAGATGACAGATGTG-3′; for AtKSS2, primers F34 5′-CGCGGATCCTTCGATGGCGCCATTGCTCAG-3′ and R210 5′-CCCGAATTCTTATGACTTCCCATCTTCAGC-3′; for AtKSS3, primers F210 5′-CGCGGATCCAAAAGGGGATTGTATGAGGGAC-3′ and 3HAtKSS 5′-CCGGAATTCCGTTAAGCAGATCCAAACTC-3′; for AtKSS12, primers 5HAtKSS60 and R210; for AtKSS23, primers F34 and 3HAtKSS. The chimeric AtKSS truncated of the domain 2, AtKSS13 (aa 1 to 34 and 211 to 523) was obtained by PCR using the QuickChange™ site-directed mutagenesis kit (Stratagene, CA, USA), the full length AtKSS in pGEX-4T-1 as substrate and the following primers: F-N-AAA 5′-GGTCCCTCATACAATCCCCTTTTGAAGAAGATGACAGATGTGTCATAGG-3′ and R-N-AAA 5′-GGTCCCTCATACAATCCCCTTTTGAAGAAGATGACAGATGTGTCATAGG-3′. All sequences were verified by sequencing. All GST−AtKSS proteins were expressed overnight at 15 °C in Rosetta (DE3)pLysS bacteria strain (Novagen-Merck Biosciences, Darmstadt, Germany) except GST−AtKSS23 that was expressed in Rosetta-gami (DE3)pLysS bacteria (Novagen). Mid-log bacterial culture (0.6 OD) were induced with 1 mM IPTG and allowed to grow overnight at 15 °C. Cells were pelleted (6000 × *g*, 15 min, 4 °C) and the pellet of bacteria was resuspended in cold lysis buffer (20 mM Tris, pH 7.4, 150 mM NaCl, 1 mM DTT, 1% Triton X-100) and sonicated. The clarified lysate was applied on a glutathione Sepharose

4B column (Amersham Pharmacia Biotech) and proteins were purified according to the manufacturer's procedures. Briefly, the column was extensively washed with 20 mM Tris, pH 7.4, 100 mM NaCl, 1 mM DTT, and the proteins were eluted in the elution buffer (20 mM Tris, pH 7.4, 100 mM NaCl, 1 mM DTT, 50 mM reduced glutathione). Samples were applied to a PD-10 column (Amersham Pharmacia Biotech) equilibrated in the storage buffer (20 mM Tris, pH 7.4, 100 mM NaCl, 1 mM DTT) to remove glutathione. Purified proteins were frozen in liquid nitrogen in the presence of 10% (v/v) glycerol and stored at $-80\,^\circ$C.

2.3. Expression of AtKSS in vivo

For transient expression in onion epidermal cells, full-length AtKSS and truncated AtKSS were cloned into the pOL-LT plasmid [25], under the control of a double strong

$$[\text{KMT}] = \frac{\left(K_{\text{d}} + [\text{MT}_{\text{tot}}] + [K_{\text{tot}}] - \sqrt{\left(K_{\text{d}} + [\text{MT}_{\text{tot}}] + [K_{\text{tot}}]\right)^2 - 4[\text{MT}_{\text{tot}}][K_{\text{tot}}]}\right)}{2}$$

35S promoter and upstream the DsRed2 fluorophore (Clontech, BD Biosciences, NJ, USA). Cells were transformed by bombardment with DNA-coated gold beads as described [26]. Cells were observed 12 to 25 h after transformation using a Leica TCS-SP2 confocal microscope (Leica Microsystems, Wetzlar, Germany). DsRed2 fluorophore was visualized under the following illumination conditions: 543 nm excitation, 580 to 620 nm emission.

2.4. Microtubule cosedimentation assays

Tubulin was purified from beef brain according to [27]. Taxol-stabilized microtubules were prepared using a procedure adapted from [28] according to the recommendations described at the web site of Tim Mitchison's laboratory (http://mitchison.med.harvard.edu/protocols/poly.html). For quantification, 10 µl of taxol-stabilized microtubules were depolymerized for 10 min at 4 $^\circ$C in 90 µl of cold depolymerizing buffer (50 mM KCl, 5 mM CaCl$_2$, 1 mM DTT in cold assembly buffer). The concentration of tubulin dimers was calculated using the absorbance of the sample at 280 nm and an extinction coefficient of 115,000 M^{-1} cm^{-1}. Considering the quantification procedure, the amount of taxol-stabilized microtubules used in the assays is indicated as concentrations of tubulin dimers (Figs. 2 and 3). To limit adsorption of AtKSS on plastic surfaces, all Eppendorf tubes and tips were siliconized [29]. To identify the domains of AtKSS involved in microtubule binding, taxol-stabilized

microtubules (0 to 3 µM) were incubated for 20 min at 25 $^\circ$C with 0.4 µM of the different GST-tagged truncated AtKSS in Binding Buffer (20 mM Hepes pH 7.2, 2 mM MgCl$_2$, 0.1 mM EGTA, 20 µM taxol, 0.5 mg/ml casein). Reactions (50 µl) were spun through a glycerol cushion (30% (v/v) glycerol in binding buffer) for 5 min at 100,000 × g as described [30]. Supernatant and the resuspended microtubule pellet were analyzed by Western blot using an anti-GST antibody and the ECL kit (Amersham Pharmacia Biotech). For K_{d} determination, 1 µM of taxol-stabilized microtubules and various concentrations of AtKSS constructs (from 0 to 5 µM) were used in the assays. The amount of AtKSS constructs free and bound to microtubules were determined by scanning Coomassie blue-stained gels and comparing the intensities with standards that were loaded on the same gel using NIH-image software (http://rsb.info.nih.go/nih-image/). The amount of AtKSS bound to microtubules is described by

where [KMT] is the concentration of AtKSS bound to microtubules, [MT$_{\text{tot}}$] and [K_{tot}] are the total concentrations of tubulin dimers and AtKSS respectively. For K_{d} calculation, data were analyzed using Kaleidagraph (Synergy Software, PA, USA).

2.5. Microtubule-severing assays

Severing of microtubules by AtKSS was either followed by video-microscopy or by spectrofluorimetry. For the video-microscopy assays, tubulin dimers were coupled to carboxyfluorescein succinimidyl ester (Molecular Probes, Eugene, OR, USA) according to [27]. Microscope-based severing assays were performed using previously published procedures [17]. DAPI (4,6-diamidino-2-phenylindole)-severing assays were performed as described previously [12]. Taxol-stabilized microtubules (1 µM) were incubated in a solution containing 20 mM Hepes, pH 7.5, 2 mM MgCl$_2$, 0.1 mM EGTA, 10 µM DAPI, 1 mM ATP. Reactions took place at 22 $^\circ$C in 100-µl samples, and started with the addition of 0.04 µM AtKSS. Fluorescence intensity was measured (excitation wavelength 360 nm; emission wavelength 460 nm) using a flx-Xenius spectrofluorimeter (Safas, Monaco).

2.6. ATPase assays

ATPase assays were performed as already described [17]. Briefly reactions (200 µl) took place at room temperature in

ATPase buffer (25 mM Aces pH 6.9, 2 mM potassium-EDTA, 1 mM 2-mercaptoethanol, 1 mM ATP, 2 mM phosphoenol pyruvate, 0.25 mM NADH, 5 µg/ml pyruvate kinase, 3 µg/ml lactate dehydrogenase), and started by the addition of 1 µM AtKSS constructs, in the absence or in the presence of 0.25 µM taxol-stabilized microtubules. In this reaction, ATP hydrolysis is coupled to the oxidation of NADH, which was monitored at 340 nm on a UV mc2® spectrophotometer (Safas, Monaco).

2.7. Electron microscopy

AtKSS was purified from insect cells as previously described [17]. Specimens at a concentration of 0,1 mg/ml were imaged by negative stain electron microscopy using a JEOL 1200 EXII microscope operating at 100 kV and a nominal magnification of 40,000×. The stain used was sodium silicotungstate.

2.8. Gel filtration chromatography

Gel filtration of katanin constructs was performed on a fast protein liquid chromatography system with a Superdex™ 200 HR 10/30 column (Amersham Pharmacia Biotech). Column equilibration and chromatography were performed in column buffer (20 mM Tris pH 8, 0.1 M KCl, 2 mM MgCl$_2$, 1 mM DTT). The column was calibrated with the following molecular mass standards: ribonuclease A (13.7 kDa), ovalbumin (43 kDa), albumin (67 kDa), aldolase (158 kDa), catalase (232 kDa), ferritin (440 kDa), Dextran Blue 2000 (Amersham Pharmacia Biotech).

2.9. Chemical cross-linking

The zero-length chemical cross-linker 1-ethyl-3-(3-dimethylaminopropyl) carbodiimide hydrochloride (EDC), along with N-hydroxysuccinimide (NHS) were obtained from Pierce (Rockford, IL, USA). Stock solutions of 100 mM EDC and NHS were made fresh in dry DMSO immediately before use. Purified AtKSS proteins (20 µg) were incubated with 1 mM EDC and 1 mM NHS at room temperature. After 10 min, 1 mM of EDC and NHS were again added to the samples. After 20 min the reaction was stopped by the addition of 9 mM glycine. The cross-linked AtKSS constructs were observed by Coomassie blue-stained gels and Western blots.

3. Results

3.1. Identification of the AtKSS microtubule-binding domain

We previously showed that AtKSS binds microtubules in vitro [17]. In a first step to understand the molecular mechanisms by which the plant katanin interacts with microtubules, we analyzed the functions of the domains of AtKSS. On the basis of the amino acid sequence alignment of AtKSS (accession number AF048706) with other known p60s

(Caenorhabditis elegans, accession number S47861; Chlamydomonas reinhardtii, accession number AAF12877; Drosophila melanogaster, accession number AAF34687; Homo sapiens, accession number AAC25114; Strongylocentrotus purpuratus, accession number AAC15706; Xenopus laevis, accession number AAD53310), we distinguished three domains (Fig. 1A). The first domain AtKSS1 corresponds to the 34 first amino acids. This short domain is highly conserved with vertebrate's p60s (AtKSS1 has 85% sequence similarity with human and Xenopus sequences). The domain AtKSS2 (amino acids 35 to 210, underlined in Fig. 1A) delimits an intermediate domain with no significant sequence similarity with known p60s. AtKSS3 (amino acids 211 to 523) delimits a large C-terminus ATPase domain, which is well conserved among all p60s (80% sequence similarity with Caenorhabditis, Drosophila, human, and Xenopus sequences). The proteins corresponding to these domains were produced in fusion with GST (GST−AtKSS1, GST−AtKSS2, GST−AtKSS3), as well as AtKSS deleted of one domain (GST−AtKSS12, GST−AtKSS13, GST−AtKSS23; Fig. 1B and C). It has to be noted that whatever expression and purification conditions we used, samples of GST−AtKSS23 contained a C-terminus truncated GST−AtKSS23 (Fig. 1C, lane "23", lower band). As these two proteins can form hetero-oligomers (see results on katanin oligomerization), we could not separate them in native conditions. When purified in denaturing conditions and further refolded, the renatured full-length GST−AtKSS23 could hydrolyze ATP, but this ATPase activity was not stimulated by microtubules. For these reasons, GST−AtKSS23 we used in this study corresponds to a mixture of the two proteins.

In order to identify the microtubule-binding domain of AtKSS, GST−AtKSS constructs were added to taxol-stabilized microtubules. After centrifugation, analysis of the supernatants and pellets showed that both GST−AtKSS12 and GST−AtKSS2 co-sedimented with microtubules, whereas neither the short N-terminus domain (GST−AtKSS1) nor the ATPase domain (GST−AtKSS3, GST−AtKSS13) interacted with microtubules (Fig. 2). These results indicate that amino acids 35 to 210 of AtKSS are involved in the interaction of AtKSS with microtubules in vitro.

3.2. Affinity of the microtubule-binding domain of AtKSS for microtubules in vitro and in vitro

We performed co-sedimentation assays with microtubules to evaluate the dissociation equilibrium constant of the GST−AtKSS2 and GST−AtKSS12 (Fig. 3). We calculated an apparent K_d of 5.10 ± 1.86 µM for GST−AtKSS2 and 6.87 ± 1.54 µM for GST−AtKSS12. The apparent K_d of GST−AtKSS12 and unfused AtKSS12 had similar values (6.87 µM for GST−AtKSS12 versus 18.03 µM ± 10.14 µM for AtKSS12), showing that in our experimental conditions GST did not significantly interfere with the binding of the proteins to microtubules. These results show that AtKSS binds microtubules with a low affinity, and that the N-terminus part of AtKSS (domain 1) is not involved in the binding of the protein to microtubules in vitro.

A

```
Hs  ....................MSLLMISENVKLAREYALLGNYDSAMVYYQGVLDQMNKYLYSVKDTYLQQKWQQVWQEINVEAKHVKDIMKTLESF  76
Xl  ....................MSLLMISENVKLAREYALLGNYDSAMVYYQGVLDQMNKYLYSVKDTFLQQKWQQVWQEINMECKHVKDIMSTLEGF  76
Sp  ....................MSVDEICENTKMGREYALLGNYETSLVYYQGVLQQIQKLLTSVHEPQRKHQWQTIRQELSQEYEHVKNITKTLNGF  76
Dm  MSITLLRGGKQKTTTCVGMTVMAKTTFEEICENAKLARDMALTGNYDSACIYYEGLQGLLARQLKATADPLRKGKWSMINQQISQEHAKIKAIQRTLQDI 100
At  ....................MVGSSNSLAGLQDHLKLAREYALEGSYDTSVIFFDGAIAQINKHLNTLDDPLARTKWMNVKKAIMEETEVVKQLDAERRAF  81
Cr  ....................MGGADVQAITIAVTTGRDCAMSGDYSAGCTYYENAVELITRYVRTLGDPHAIRQWSALLKEVQDEHSSVRQCDKEARGM  79
Ce  ....................MNGDVQSVIRGYLERAQVAKTMSDAGRWNEAGDLLRQLMTDVKSCKISASNRDEHDARNTFLRALEANLKLVQQNVRDEDDL  82
```

```
Hs  KLDSTP.........LKAAQH..................DLPASEGEVVWSMPVP......VERRPSP......GPRKRQSSQYSDPKS.....HGNRPSTT 133
Xl  KLDSSP.........VKTTQH..................EFPSHDGEVVWSLPVP......VERRPSP......GPRKRQSVQCNDNKS.....HNNRFSAA 133
Sp  KSEPAAP.........EPAPNHRAAPFSHHQHAAKPAAAEPARDPDVWPPTP......VDHRPSPPYQ...RAARKDPPRRSEPSK.....PANRAPGN 153
Dm  SLDLQSTKFAHKLRHQLSEESTTSKDPSAWFKPDPDIWTPPPKDPDVWGPPKPPPTTQAVGRRAAPNNRRTTPATQNSRPSSTIPQS.....TARNGPAS 195
At  KEAPTGRR.....AASPPINTKSSFVFQPLDEYPTSSGGGPMDDPDVWRPTR....DVTSRPRARAG...QTGTRKSPQDGAWARG.....PTTRTGPA 164
Cr  RVYDSVAR..SNSYPEMNDPRGSAAYDDGYRQPIVVCHNSGQEDPMVWRPPTRGEGRSGAPARGAPPPRARSSQDDNKLPSWANNNNGGGGGPPARGNAA 177
Ce  HEAMTRQS................GSPEPPADPDVWSKPSP..................PLPSSSKFGATKKG.....VGAAGPRP 129
```

```
Hs  VR.VHRSSAQNVHNDRGKA....VRCREKKEQNKGREEKNKSPAA...............VTEPETNKFDST.GYDKDLVEALERDIISQNP.NVRWDD 210
Xl  AKGPNLPSARNANNVKMKP....VRAREKKD...ALIKNKSSAD...............VSETEVKRFDGS.GYDKDLIEALERDIISQNP.NIRWDD 207
Sp  DRGGRGPSDRRGDARSGGGGRGGARGSDKDKNRGGKSDKDKKAPS...........GEEGDEKKFDPA.GYDKDLVENLERDIVQRNP.NVHWAD 235
Dm  TRNSRNSTSATAPSGGARTTNGRAGGRKLSTSNTNEARDDDSTAAGNNGGAAGDGENGDPQAAQEEERKFQPNNHIEAELVDILERDILQKDP.KVRWSD 294
At  SRGGRGGATSKSTAGARSS....TAGKKGAASKSNKAESMNGDAE...........DGKSKRGLYEGP...DEDLAAMLERDVLDSTP.GVRWDD 240
Cr  GPSGRGAGSAPRRPTGNAPAGNAAAGGSYDRPWRQNMQGKQGAAGPGGKPGDKGS.......AGEKAKKQYSGP...DQELAAMLERDIVDQGT.SVKWDD 266
Ce  REISKSTSSMSTNPADVKP...............ANPTQGILP...........QNSAGDSFDAS.AYDAYIVQAVRGTMATNTENTMSLDD 194
```

```
Hs  IADLVEAKKLLKEAVVLPMWMPEFFKGIRRPWKGVLMVGPPGTGKTLLAKAVATECKTTFFNVSSSTLTSKYRGESEKLVRLLFEMARFYSPATIFIDEI 310
Xl  IADLEEAKKLLKEAVVLPMWMPEFFKGIRRPWKGVLMVGPPGTGKTLLAKAVATECKTTFFNISSSTLTSKYRGESEKLVRLLFEMARFYAPTTIFIDEI 307
Sp  IAGLTEAKRLLEEAVVLPLWMPDYFKGIRRPWKGVLMVGPPGTGKTMLAKAVATECGTTFFNVSSASLISKYHGESEKLVRLLFEMARFYAPSTIFIDEI 335
Dm  IADLHDAKRLLEEAVVLPMPDYFKGIRRPWKGVLMVGPSGTGKTMLAKAVATECGTTFFNVSSATLISKYRGESEKMVRLLFEMARDLAPSMIFIDEV 394
At  VAGLSEAKRLLEEAVVLPLWMPEYFQGIRRPWKGVLMFGPPGTGKTLLAKAVATECGTTFFNVSSATLASKWRGESERMVRCLFDLARAYAPSTIFIDEI 340
Cr  IAGLEEAKRVLNEALVLPMIMPDFFTGIRRPVKGVLLFGPPGTGKTMLAKAAATETSCTFFNVSSATLASKYRGESERMVRILLFEMARDLAPSMIFIDEV 366
Ce  IIGMHDVKQVLHEAVTLPLLVPEFFQGLRSPWKAMVLAGPPGTGKTLIARAIASESSTFFTVSSTDLSKWRGDSEKIVRLLFELARFYAPSIIFIDEI 294
```

```
Hs  DSICSRRGTSEEHEASRRVKABLLVQMDGVGGTSENDDPSK.......MVMVLAATNFPWDIDEALRRRLEKRIYIPLPSAKGREELLRISLRELELAD 402
Xl  DSICSRRGTSEEHEASRRVKAELLVQMDGVGGASENEDPSK.......MVMVLAATNFPWDIDEALRRRLEKRIYIPLPSAKGREELLRINLKELELAD 399
Sp  DSICSRRGTSGSEHEAKVKSELLIQMDGVSGPSAGEESSK.......MVMVLAATNFPWDIDEALRRRLEKRIYIPLPEIDGREQLLRINLKEVPLAD 427
Dm  DSLCSRRGSESEHEASRRVKSELLVQMDGVAR....EEQAK.......VIMVLAATNFPWDIDEALRRRLEKRIYIPLPSDEGREALLKINLREVKVDD 482
At  DSLCNSRGGSGEHESSRRVKSELLVQMDGVSNTATNEDGSRK.......IVMVLAATNFPWDIDEALRRRLEKRIYIPLPDFESRKALININLRTVEVAS 433
Cr  DSLCSQRGTANEHEASRRVKTELLTQVDGVHGSEKDKEPGPDGEPPAPKHVFVLAATNFPWDIDEALRRRLEKRVYIPLPGQAQRLQLLKINLRDVAVAP 466
Ce  DTLGGQRGNSGEHEASRRVKSEFLVQMDGSQNKFDSRR...........VFVLAATNIPWELDEALRRRFEKRIFIPLPDIDARKKLIEKSMEGTPKSD 382
```

```
Hs  DVDLASIAENMEGYSGADITNVCRDASLMAMRRRIEGLTPEEIR.NLSKEEMHM...PTTMEDFEMALKKVSKSVSAADIERYEKWIFEFGSC 491
Xl  DVNIECIAENMDGYSGADITNVCRDASLMAMRRRIEGLTPEEIR.NLSRDDMHM...PTTMEDFEMALKKVSKSVSASDIEKYEKWIFEFG.. 486
Sp  DIDDLKSIAEKMDGVSGADITNVCRDASMMAMRRRIQGLREIR.HIPKEELNQ...PSTPADFLLALQVSKSVGKEDLVKYMAWMEEFGSV 516
Dm  SVDLTYVANELKGYSGADITNVCREASMMSMRRKIAGLTPEQIR.QLATEEVDL..PVSNKDFNEAMSRCNKSVSRADLDKYEKWMREFGSS 571
At  DVNIEDVARRTEGYSGDDLTNVCRDASMNGMRRKIAGKTRDEIK.NMSKDDISND..PVAMCDFEEAIRKVQPSVSSSDIEKHEKWLSEFGSA 523
Cr  DVNLEAVAGOMDGYSGDDITNVCRDAAMNGMRRLVAGKTPAEIK.ALREAGMTGGQEPITSDDFREALRKINPSVSKEDIKRHEEWLSVFGST 558
Ce  EINYDLAARTEGFSGADVVSLCRTAAINVLRRYFRYDTKSLRGGELTAAMESLKAELVRNIDFEAALQAVSPSAGPDTMLKCKEWCDSFGAM 475
```
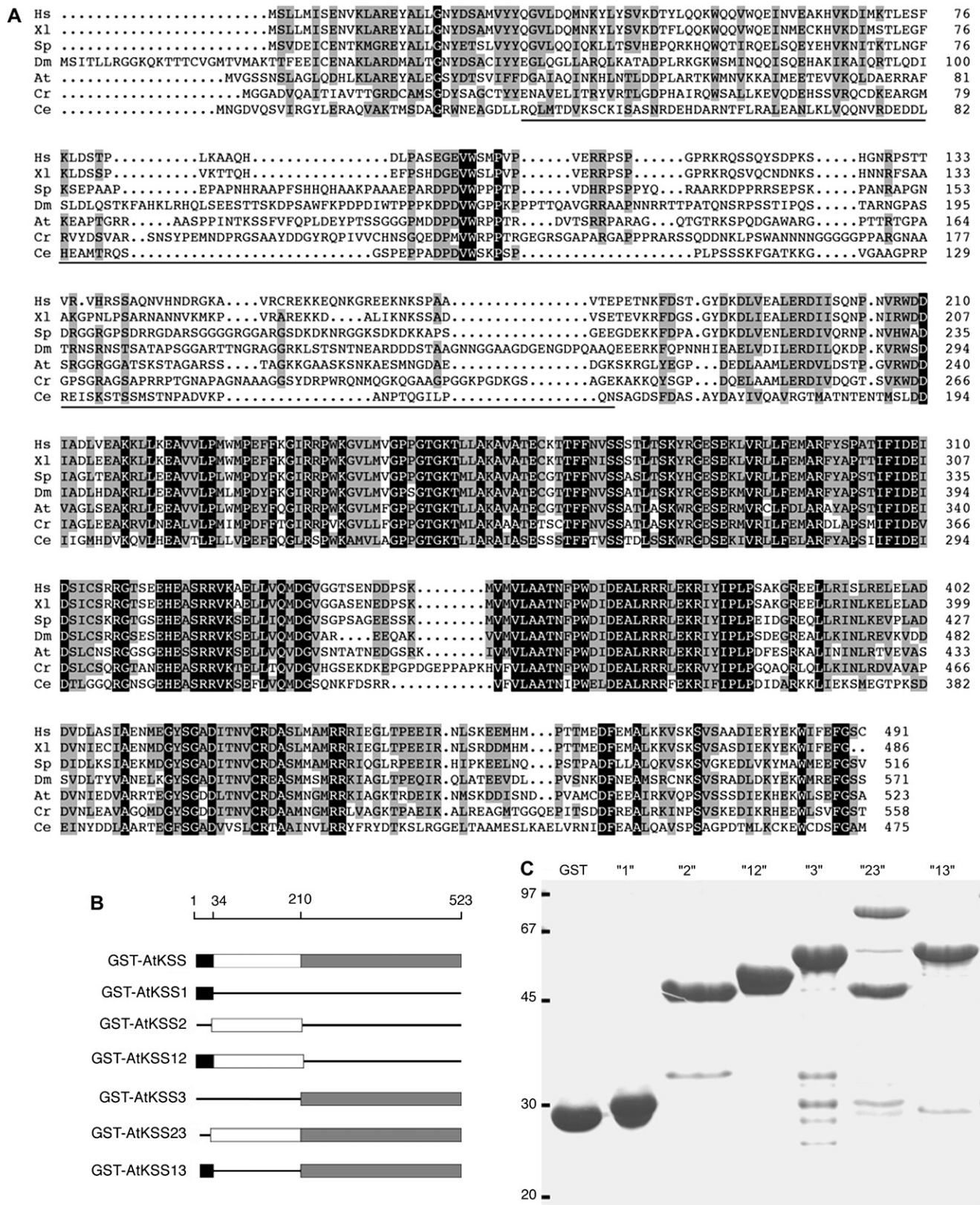
B

C

Fig. 1. AtKSS constructs used in this study. (A) Alignment of amino acid sequences of most known katanin p60 including *Homo sapiens* (Hs), *Xenopus laevis* (Xl), *Strongylocentrotus purpuratus* (Sp), *Drosophila melanogaster* (Dm), *Arabidopsis thaliana* AtKSS (At), *Chlamydomonas reinhardtii* (Cr) and *Caenorhabditis elegans* (Ce). Identical and similar amino acids are highlighted in black and gray respectively. Dashes represent gaps. The domain 2 is underlined. (B) Diagram of the different AtKSS constructs corresponding to combination of domain 1 (aa 1 to 34, black box), domain 2 (aa 35 to 210, white box) and domain 3 (aa 211 to 523, gray box). C, Coomassie blue-stained SDS–PAGE gel of the purified AtKSS constructs. From left to right, GST, GST–AtKSS1 ("1"), GST–AtKSS2 ("2"), GST–AtKSS12 ("12"), GST–AtKSS3 ("3"), GST–AtKSS23 ("23"), GST–AtKSS13 ("13"). Masses of molecular markers are indicated in kDa.
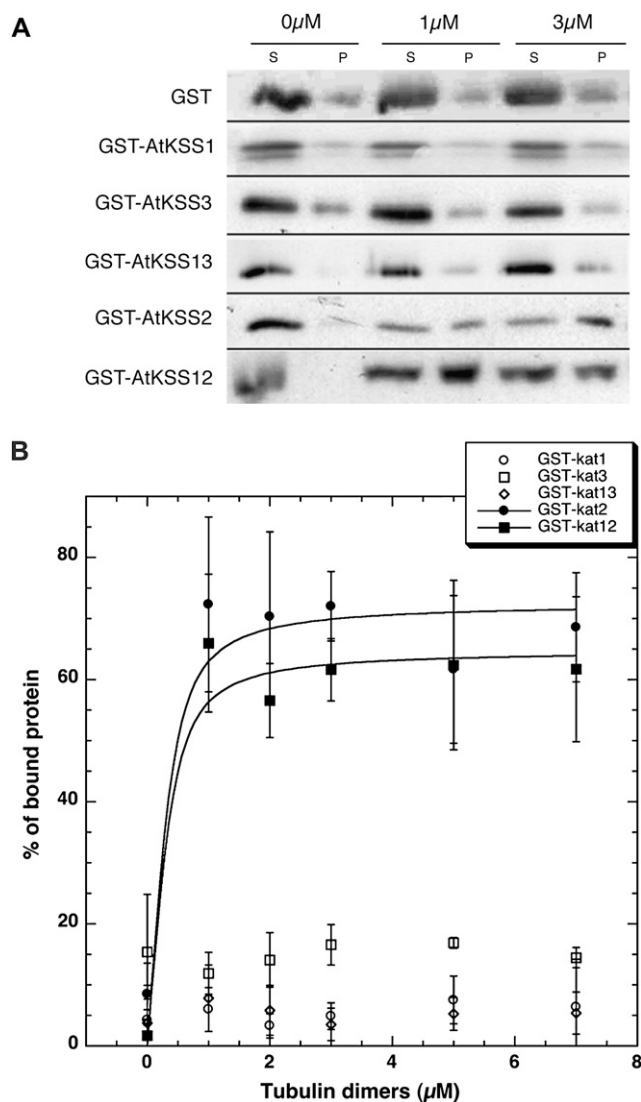
A

B

Fig. 2. Binding of AtKSS constructs to microtubules *in vitro*. 0.4 μM of GST–AtKSS constructs were incubated with various amount of microtubules. Samples were centrifuged to pellet microtubules and the amount of GST–AtKSS proteins bound to microtubules was evaluated by densitometry. (A) Western blot of supernatant (S) and pellet (P) of GST–AtKSS proteins probed with GST antibodies. Concentrations of microtubules used in each assay (indicated as the concentration of tubulin dimers) are indicated. (B) Results are expressed as percentage of total GST–AtKSS constructs that pelleted with microtubules versus tubulin dimers concentration. Vertical bars represent standard deviation of a least three repeats.

We wondered whether the microtubule-binding domain of AtKSS interacts with microtubules in vivo, where microtubules are covered with microtubule-associated proteins. We transiently expressed AtKSS12 or AtKSS2 fused to DsRed in onion epidermal cells. Sixteen hours after transformation, the AtKSS12-DsRed (Fig. 4A) and AtKSS2-DsRed were detected along filaments. We did not detect any difference between the localization of AtKSS12 and AtKSS2 in vivo. Transformed cells were treated with 20 μM oryzalin, a potent plant microtubule destabilizer. This concentration of oryzalin is sufficient to depolymerize all microtubules detectable at

the light microscope level in vivo [31]. After 20 min of incubation, almost all the stained filaments had disappeared (Fig. 4B–D). These results show that the domain of AtKSS delimited by the amino acids 35 to 210 binds microtubules in living cells.

3.3. Oligomerization of AtKSS

In order to determine whether AtKSS is able to form oligomers, we examined the structure of AtKSS molecules at the electron microscopy level. AtKSS appeared as irregular rings of 25–30 nm diameter composed of globular subunits (Fig. 5A–C). Rings of AtKSS often contained a crack radiating outward. These rings are very similar to hexamers of animal p60 [12].

To identify domains of AtKSS that may be involved in the oligomerization, we studied the oligomeric state of the different AtKSS constructs. First, the molecular mass of the different katanin constructs was estimated by gel filtration. The N-terminus part of katanin (GST–AtKSS1), the ATPase domain of katanin (GST–AtKSS3), and the chimeric protein composed of these two domains (GST–AtKSS13) were eluted from the column as dimers (Table 1). Because GST exists as a dimer in its native state [32], and because in our experimental conditions GST was eluted as a dimer (Table 1), we concluded that dimers of GST–AtKSS1, GST–AtKSS3 and GST–AtKSS13 resulted from the dimerization of GST. In contrast the microtubule-binding domain of katanin, either alone (GST–AtKSS2) or combined to the N-terminus domain (GST–AtKSS12) was eluted as trimers. We also performed cross-linking experiments with the different GST constructs using the zero-length cross-linker EDC together with NHS. These experiments could not be done with GST–AtKSS2, as the protein is not stable at room temperature. Incubation of GST–AtKSS12 with the cross-linker yielded to
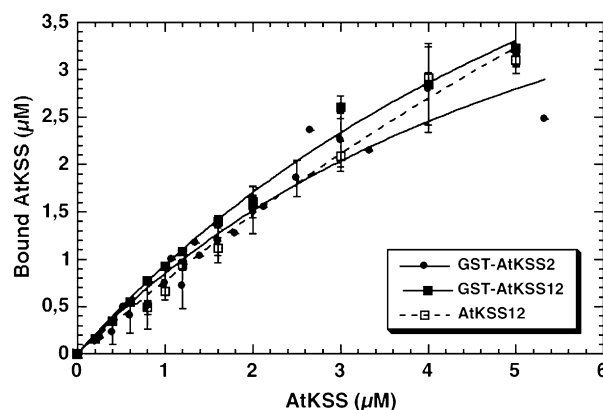

Fig. 3. Affinity of the microtubule-binding domain of AtKSS for microtubules. The amount of AtKSS12 (open square, dotted line), GST–AtKSS12 (filled square, solid line) and GST–AtKSS2 (filled circle, solid line), are plotted as a function of the total amount of AtKSS used for co-sedimentation assays with microtubules. The fitting curve was defined using the equation given in Section 2, and was used to determine the K_d of AtKSS12 (18.03 μM), GST–AtKSS12 (6.87 μM) and GST–AtKSS2 (5.10 μM) for microtubules. Vertical bars represent standard deviation of at least three repeats.
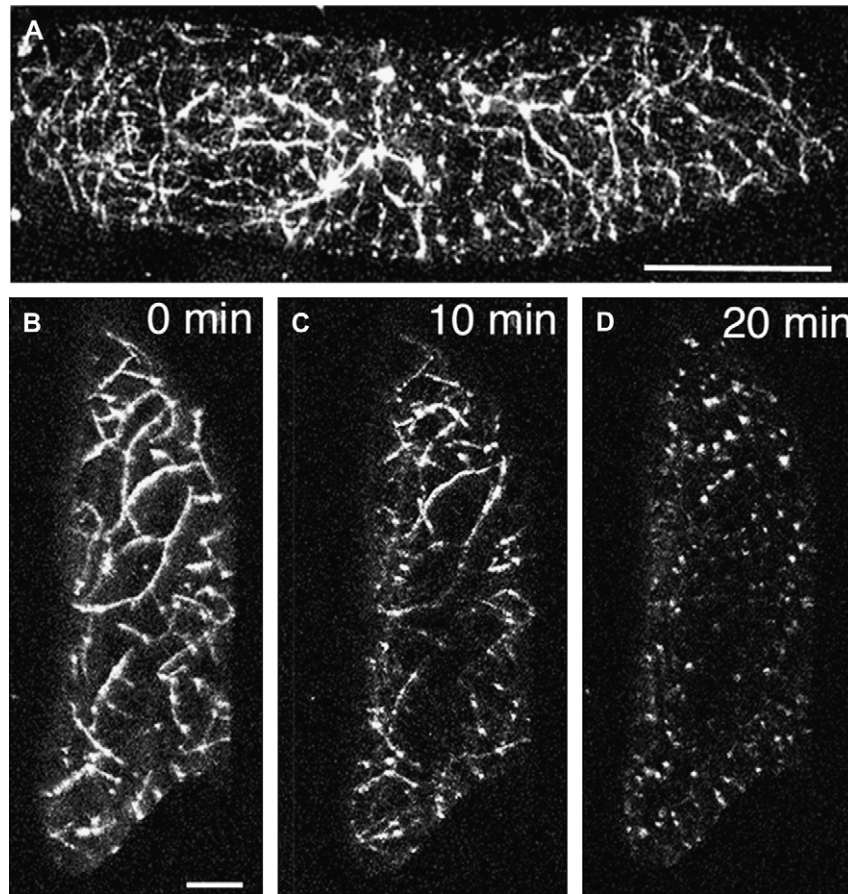
Fig. 4. Localization of AtKSS12 *in vivo*. (A) Onion epidermal cell transiently expressing AtKSS12-DsRed and observed 16 h after bombardment. A dense and disorganized network of filaments is detected in the cortex of the cell. (B–D) Time-lapse observation of an onion cell expressing AtKSS-DsRed and treated with 20 µM oryzalin, a microtubule-depolymerizing drug, for 0 min (B), 10 min (C) and 20 min (D). After 20 min of treatment, no microtubules were observed.

a band of an apparent molecular mass of 160 kDa (Fig. 5D). This result suggests that AtKSS12 forms trimers. None of the chimeric proteins lacking the microtubule-binding domain (GST alone, GST–AtKSS1, GST–AtKSS3 (data not shown) or GST–AtKSS13 (Fig. 5E)) formed oligomers. Trimers of AtKSS12 without GST were also observed after cross-linking (Fig. 5F). All together these data suggest that AtKSS oligomerizes into a ring-shaped oligomers, and that the microtubule-binding domain of AtKSS is involved in the oligomerization process.

3.4. ATPase and microtubule-severing activity of katanin

We studied the ATPase activity and severing activity of the different domains of katanin. From all the chimeric AtKSS we studied, only those containing domain 3 (GST–AtKSS13, GST–AtKSS23 and GST–AtKSS3) hydrolyzed ATP (Fig. 6A). GST–AtKSS2 and GST–AtKSS12 had no detectable ATPase activity. Noticeably, the ATPase activity of GST–AtKSS23 was stimulated by microtubules, as observed for baculovirus-expressed full-length AtKSS [17]. Hydrolysis of ATP by GST–AtKSS13 and GST–AtKSS3 was not stimulated by microtubules. These data are in agreement with our results

showing that the ATPase domain of katanin is not able to interact with microtubules.

We also analyzed the microtubule-severing activities of different katanin constructs using spectrofluorimetry and video-microscopy assays. We observed that the chimeric katanin containing the microtubule-binding domain and the ATPase domain (GST–AtKSS23) destabilized microtubules in vitro (Fig. 6B,E,F). In contrast, neither GST–AtKSS1, nor the microtubule-binding domain alone (GST–AtKSS2) or fused to the domain 1 (GST–AtKSS12), nor the ATPase domain alone (GST–AtKSS3) severed microtubules in vitro. Our data did not allow us to quantitatively compare the severing activities of the GST–AtKSS23 and the full-length katanin and thus to determine if the presence of the short NH_2-terminal domain (AtKSS1) modulates katanin's activities in vitro. Our results show that the microtubule-binding domain and the ATPase domain are sufficient for katanin to sever microtubules in vitro.

4. Discussion

Up to now, data obtained from the analysis of four AtKSS mutants [18–20,22,23] and from the induced expression of AtKSS in arabidopsis plants [24] clearly indicate that AtKSS is required for a proper organization of cortical microtubules
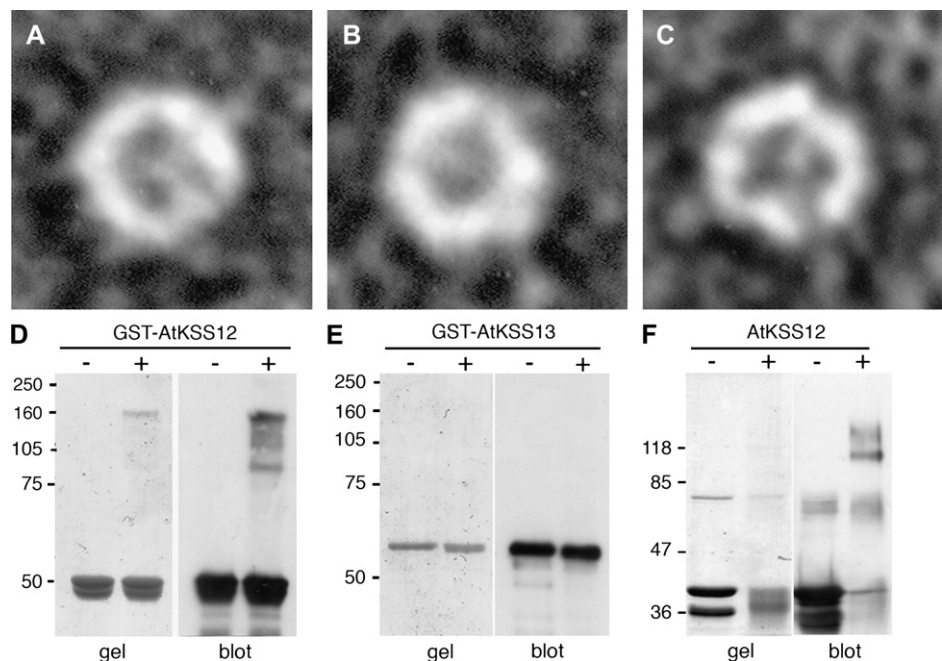
Fig. 5. Structure and oligomerization of AtKSS. (A–C) Electron micrographs of AtKSS purified from baculovirus-infected insect cells. Rings are 25–30 nm diameter. (D–F) Cross-linking of GST–AtKSS12, GST–AtKSS13 and AtKSS12. GST–AtKSS12 (D), GST–AtKSS13 (E) and AtKSS12 (F) were incubated in the absence (lanes −) or in the presence (lanes +) of cross-linker molecules. Samples were analyzed by Coomassie blue-stained SDS–PAGE (gel) and by Western blot an anti-GST antibody (GST–AtKSS12 and GST–AtKSS13) or anti-AtKSS antibodies (AtKSS12). Masses of molecular markers are indicated in kDa. Bar = 20 μm.

in expanding plant cells. But how katanin achieves this function is still unknown. In this study, we examined some of the molecular properties of katanin, including its interaction with microtubules and its ability to form oligomers.

Our data show that amino acids 35 to 210 of AtKSS are sufficient for AtKSS to bind microtubules both in vitro and in vivo. Noticeably plant and animal catalytic subunits of katanin bind microtubules via the same domain (domain 2, see Fig. 1A) and with a comparable K_d (this study, [13,30]). This may be due to the fact that although the amino-acid sequences of plant and animal microtubule-binding domains of katanin are poorly conserved, they are enriched in basic amino acids that can interact with the acidic tubulin surface.

We found that besides mediating the interaction of katanin with microtubules, the microtubule-binding domain of AtKSS allows intermolecular interactions between katanin subunits.

Indeed, the microtubule-binding domain of AtKSS oligomerizes into trimers and AtKSS forms rings similar in size and in shape to sea urchin katanin [12]. These results suggest that the microtubule-binding domain is involved in the oligomerization of katanin. It has been shown that the microtubule-severing activity of animal katanin is correlated with its ability to oligomerize into a ring-shaped hexamer [13]. Assuming that the active AtKSS is also a hexamer, we propose that the oligomerization of the catalytic subunit of katanins takes place in at least two steps: the formation of a trimer and then the addition of two trimers to form a hexamer. More detailed structural data are now required to understand how katanin subunits interact to form a hexamer, and to evaluate the role of the catalytic state of the ATPase domain in this process.

Our data did not allow us to specify a function to the N-terminus of AtKSS (AtKSS1). This domain does not bind microtubules by itself, neither does it interfere with the interaction of the microtubule-binding domain with microtubules, as K_d values of GST–AtKSS2 and GST–AtKSS12 were similar. It is probably not essential for the oligomerization of AtKSS as GST–AtKSS23 fragments microtubules. It is possible that this domain, although not necessary for severing activity of AtKSS, favors one or several steps of the microtubule-binding/oligomerization/ATP hydrolysis cycle of AtKSS, and that the procedures we used were not sensitive enough to detect such a fine regulation. The N-terminus part of AtKSS may also be involved in the recruitment of AtKSS-regulatory proteins, as has been shown for animal katanin [30]. AtKSS-interacting proteins have recently been identified by two-hybrid
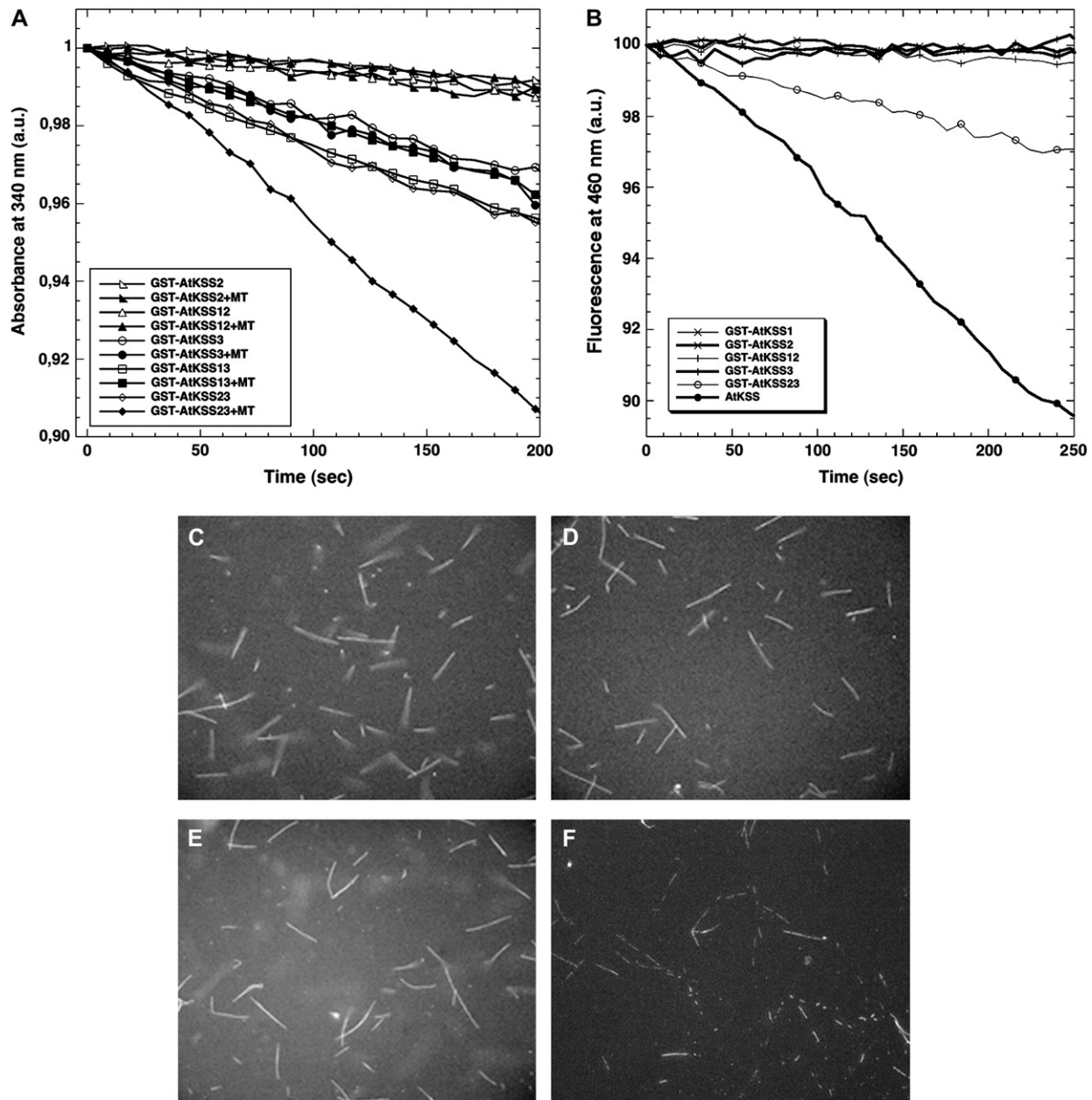
Table 1
Number of oligomers of the different AtKSS constructs

	Predicted molecular mass[a] (Da)	Estimated molecular mass[b] (Da)	No. of oligomers
GST	27.783	49.477	1.78
GST–AtKSS1	31.485	57.464	1.83
GST–AtKSS3	62.810	102.058	1.63
GST–AtKSS13	66.512	147.711	2.22
GST–AtKSS2	46.273	126.233	2.73
GST–AtKSS12	49.975	162.465	3.25

[a] Molecular masses predicted from amino acid sequence.
[b] Values calculated form the gel filtration data.

Fig. 6. ATPase and microtubule-severing activity of GST−AtKSS23. (A) ATPase activity 1 μM of GST−AtKSS2, GST−AtKSS12, GST−AtKSS3, GST−AtKSS13 and GST−AtKSS23 was followed at 340 nm in the absence (open symbols) and in the presence (black symbols) of 0.25 μM tubulin dimers. The decrease of the absorbance accompanying ATPase activity shows that GST−AtKSS23 has a basal ATPase activity (open diamonds) that is 2.7-fold stimulated by microtubules (black diamonds). GST−AtKSS13 (open squares) and GST−AtKSS3 (open circles) have a low ATPase activity that is not stimulated by microtubules (black symbols). (B) Severing of microtubules by GST−AtKSS23 followed by spectrofluorimetry at 460 nm. The decrease of the absorbance of taxol-stabilized microtubules incubated GST−AtKSS23 or with baculovirus-expressed full-length *Arabidopsis* katanin shows that these two proteins severed microtubules. Microtubules incubated with the GST−AtKSS1, GST−AtKSS2, GST−AtKSS12 and GST−AtKSS3 did not depolymerize. (C−F) Severing of fluorescent taxol-stabilized microtubules by GST−AtKSS23 observed by microscopy. Fluorescein-labeled taxol-stabilized microtubules were incubated either with the reaction buffer (C,D) or with GST−AtKSS23 (E,F). After 15 min in the presence of GST−AtKSS23, most microtubules were severed (F). Bar = 10 μm.

screen [22]. Characterization of the ability of these proteins to regulate katanin in vitro and in vivo will be of great help in the understanding of the roles of microtubule severing in higher plants.

Non-ectopic fragmentation of microtubules in plant cells implies that the activity of katanin is regulated in vivo. One way to control katanin's activity is to modulate its binding to microtubules. Several lines of evidence suggest that katanin transiently interacts with microtubules. First, anti-katanin antibodies did not detect AtKSS along microtubules [16]. Second, in our hands, co-localization of katanin with microtubules in vivo was only observed in transiently transgenic cells in which AtKSS was overexpressed after biolistic transformation (our unpublished data). Neither in transgenic *Arabidopsis* cells

expressing AtKSS in an inducible manner [24], nor in tobacco cells expressing AtKSS after agro-infiltration (our unpublished results), could we detect an interaction between katanin and microtubules. Indeed, there is only one study reporting the co-localization of AtKSS with microtubules in vivo [22]. In this work, stably overexpressed AtKSS–GFP–GUS decorates microtubules in *Arabidopsis* plants. However the functionality of the tripartite chimeric protein used in the study has been questioned by the authors. Third, the K_d value we calculated for the microtubule-binding domain of AtKSS is at least ten times higher than the K_d we estimated for plant MAP65-1b [33]. All these observations are consistent with a transient interaction of plant katanin with microtubules. The absence of co-localization of a microtubule-interacting protein with microtubules in vivo is not unique to katanin. Recent studies showed that spastin, an AAA katanin-related protein that destabilizes microtubules does not co-localized with microtubules in animal cells, whereas mutated spastin with altered ATPase activity does [34,35]. These results show that ATP hydrolysis is involved in the interaction of spastin with microtubules. Whether a comparable mechanism also affects the interaction of plant katanin with microtubules remains to be shown.

The present study provides new insights into the molecular properties of plant katanin. However many questions remain to be answered before we can fully understand the molecular mechanisms underlying microtubule severing by katanin in plants. Does katanin preferentially associate with a subset of microtubules in vivo? If so, how is this association regulated? Does it depend on the dynamic properties of microtubules, and/or on the presence of microtubule-associated proteins such as MAP65 proteins? What is the role of the homologue of the katanin-accessory protein p80? The ongoing characterization of plant microtubule-interacting proteins should soon provide insights into these challenging issues.

Acknowledgments

References

[1] B. Kost, J. Mathur, N.H. Chua, Cytoskeleton in plant development, Curr. Opin. Plant Biol. 2 (1999) 462–470.

[2] C.W. Lloyd, J. Chan, Microtubules and the shape of plants to come, Nat. Rev. Mol. Cell Biol. 5 (2004) 13–22.

[3] J. Chan, G.M. Calder, J.H. Doonan, C.W. Lloyd, EB1 reveals mobile microtubule nucleation sites in *Arabidopsis*, Nature Cell Biol. 5 (2003) 967–971.

[4] P. Dhonukshe, T.W.J. Gadella, Alteration of microtubule dynamic instability during preprophase band formation revealed by yellow fluorescent protein-CLIP170 microtubule plus-end labeling, Plant Cell 15 (2003) 597–611.

[5] S.L. Shaw, R. Kamyar, D.W. Ehrhardt, Sustained microtubule treadmilling in *Arabidopsis* cortical arrays, Science 300 (2003) 1715–1718.

[6] J. Vos, M. Dogterom, A.M.C. Emons, Microtubules become more dynamic but not shorter during preprophase band formation: a possible ''search-and-capture'' mechanism for microtubule translocation, Cell Motil. Cytoskel. 57 (2004) 246–258.

[7] T. Hashimoto, Dynamics and regulation of plant interphase microtubules: a comparative view, Curr. Opin. Plant Biol. 6 (2003) 568–576.

[8] J.C. Sedbrook, MAPs in plant cells: delineating microtubule growth dynamics and organization, Curr. Opin. Plant Biol. 7 (2004) 632–640.

[9] P.J. Hussey, T.J. Hawkins, H. Igarashi, D. Kaloriti, A. Smertenko, The plant cytoskeleton: recent advances in the study of the plant microtubule-associated proteins MAP-65, MAP-190 and the *Xenopus* MAP215-like protein, MOR1, Plant Mol. Biol. 50 (2002) 915–924.

[10] M. Sasabe, Y. Machida, MAP65: a bridge linking a MAP kinase to microtubule turnover, Curr. Opin. Plant Biol. 9 (2006) 563–570.

[11] F. McNally, R.D. Vale, Identification of katanin, an ATPase that severs and disassembles stable microtubules, Cell 75 (1993) 419–429.

[12] J.J. Hartman, J. Mahr, K. McNally, K. Okawa, A. Iwamatsu, S. Thomas, S. Cheesman, J. Heuser, R.D. Vale, F.J. McNally, Katanin, a microtubule-severing protein is a novel AAA ATPase that targets to the centrosome using a WD40-containing subunit, Cell 93 (1998) 277–287.

[13] J.J. Hartman, R.D. Vale, Microtubule disassembly by ATP-dependent oligomerization of the AAA enzyme katanin, Science 286 (1999) 782–785.

[14] K. McNally, A. Audhya, K. Oegema, F.J. McNally, Katanin controls mitotic and meiotic spindle length, J. Cell Biol. 175 (2006) 881–891.

[15] F. McNally, K. Okawa, A. Iwamatsu, R.D. Vale, Katanin, the microtubule-severing ATPase, is concentrated at centrosomes, J. Cell Sci. 109 (1996) 561–567.

[16] R.S. McClinton, J.S. Chandler, J. Callis, cDNA isolation, characterization, and protein intracellular localization of a katanin-like p60 subunit from *Arabidopsis thaliana*, Protoplasma 216 (2001) 181–190.

[17] V. Stoppin-Mellet, J. Gaillard, M. Vantard, Functional evidence for in vitro microtubule severing by the plant katanin homologue, Biochem. J. 365 (2002) 337–342.

[18] A. Bichet, T. Desnos, S. Turner, O. Grandjean, H. Höfte, *BOTERO1* is required for normal orientation of cortical microtubules and anisotropic cell expansion in *Arabidopsis*, Plant J. 25 (2001) 137–148.

[19] D.H. Burk, B. Liu, R. Zhong, W.H. Morrison, Z.H. Ye, A katanin-like protein regulates normal cell wall biosynthesis and cell elongation, Plant Cell 13 (2001) 807–827.

[20] D.H. Burk, Z.H. Ye, Alteration of oriented deposition of cellulose microfibrils by mutation of a katanin-like microtubule-severing protein, Plant Cell 14 (2002) 2145–2160.

[21] M. Webb, S. Jouannic, J. Foreman, P. Linstead, L. Dolan, Cell specification in the *Arabidopsis* root epidermis requires the activity of *ECTOPIC ROOT HAIR 3*—a katanin-p60 protein, Development 129 (2002) 123–131.

[22] T. Bouquin, O. Mattsson, H. Naested, R. Foster, J. Mundy, The *Arabidopsis lue1* mutant defines a katanin p60 ortholog involved in hormonal control of microtubule orientation during cell growth, J. Cell Sci. 116 (2003) 791–801.

[23] M. Komorisono, M. Ueguchi-Tanaka, I. Aichi, Y. Hasegawa, M. Ashikari, H. Kitano, M. Matsuoka, T. Sazuka, Analysis of the rice mutant *dwarf and gladius leaf 1*. Aberrant katanin-mediated microtubule organization causes up-regulation of gibberellin biosynthetic genes independently of gibberellin signaling, Plant Physiol. 138 (2005) 1982–1993.

[24] V. Stoppin-Mellet, J. Gaillard, M. Vantard, Katanin's severing activity favors bundling of cortical microtubules in plants, Plant J. 46 (2006) 1009–1017.

[25] P. Mollier, B. Hoffmann, C. Debast, I. Small, The gene encoding *Arabidopsis thaliana* mitochondrial ribosomal protein S13 is a recent

duplication of the gene encoding plastid S13, Curr. Genet. 40 (2002) 405−409.

[26] W. Chiu, Y. Niwa, W. Zeng, T. Hirano, H. Kobayashi, J. Sheen, Engineered GFP as a vital reporter in plants, Curr. Biol. 6 (1996) 325−330.

[27] A. Hyman, D. Drechsel, D. Kellogg, S. Salser, K. Sawin, P. Steffen, L. Wordeman, T. Mitchison, Preparation of modified tubulin, Methods Enzymol. 196 (1991) 478−485.

[28] L.D. Belmont, T.J. Mitchison, Identification of a protein that interacts with tubulin dimers and increases the catastrophe rate of microtubules, Cell 84 (1996) 623−631.

[29] J. Sambrook, E.F. Fritsch, T. Maniatis, Molecular Cloning: A Laboratory Manual, 2nd Edition, Cold Spring Harbor Laboratory Press, Cold Spring Harbor, NY, 1982.

[30] K.P. McNally, O.A. Bazirgan, F.J. McNally, Two domains of p80 katanin regulate microtubule severing and spindle pole targeting by p60 katanin, J. Cell Sci. 113 (2000) 1623−1633.

[31] M.N. Binet, C. Humbert, D. Lecourieux, M. Vantard, A. Pugin, Disruption of microtubular cytoskeleton induced by cryptogein, an elicitor of hypersensitive response in tobacco cells, Plant Physiol. 125 (2001) 564−572.

[32] X. Ji, P. Zhang, R.N. Armstrong, G.L. Gilliland, The three-dimensional structure of a glutathione S-transferase from the mu gene class. Structural analysis of the binary complex of isoenzyme 3-3 and glutathione at 2.2-A resolution, Biochemistry 31 (1992) 10169−10184.

[33] C. Wicker-Planquart, V. Stoppin-Mellet, L. Blanchoin, M. Vantard, Interactions of tobacco microtubule-associated protein MAP65-1b with microtubules, Plant J. 39 (2004) 126−134.

[34] K.J. Evans, E.R. Gomes, S.M. Reisenweber, G.G. Gundersen, B.P. Lauring, Linking axonal degeneration to microtubule remodeling by spastin-mediated microtubule severing, J. Cell Biol. 168 (2005) 599−606.

[35] A. Roll-Mecak, R.D. Vale, The drosophila homologue of the hereditary spastic paraplegia protein, spastin, severs and disassembles microtubules, Curr. Biol. 15 (2005) 650−655.